Porous Ceramic Coating for Transpiration Cooling of Gas Turbine Blade

M. Arai and T. Suidzu

A transpiration cooling system for gas turbine applications has significant benefit for reducing the amount of cooling air and increasing cooling efficiency. In this paper, the porous ceramic coating, which can infiltrate cooling gas, is developed with plasma spraying process, and the properties of the porous coating material such as permeability of cooling gas, thermal conductivity, and adhesion strength are examined. The mixture of 8 wt.% yttria-stabilized zirconia and polyester powders was employed as the coating material, in order to deposit the porous ceramic coating onto Ni-based super alloy substrate. It was shown that the porous ceramic coating has superior permeability for cooling gas. The adhesion strength of the porous coating was low only 20% compared with the thermal barrier coating utilized in current gas turbine blades. Simulation test of hot gas flow around the gas turbine blade verified remarkable reduction of the coating surface temperature by the transpiration cooling mechanism. It was concluded that the transpiration cooling system for the gas turbine could be achieved using the porous ceramic coating developed in this study.

1. Introduction

In gas turbine system utilized in an electric power plant, R&D has been done extensively to reach a high overall efficiency (Ref 1-6). Efficiency in gas turbine plant can be achieved easily by the increase of turbine inlet temperature (TIT), which also brings about the increase of metal temperature in the components of gas turbine such as a first-stage blade. In order to protect such components from the hot gas attack, thermal barrier coatings (TBCs) are applied on the surface of the blade and film cooling system is applied. Film cooling system is a well-known technology which reduces heat transfer from the hot gas to the blade surface through a boundary layer covering the blade surface by cooling air blow from the cooling holes. However, it is required to restrain the amount of cooling air ejected from the compressor in order to minimize the loss of the efficiency in the plant (Ref 7, 8). In contrast with such conventional cooling system, transpiration cooling system (Ref 9-11) is also known as one of the better cooling technologies which are combined with film cooling process and the porous wall attached onto the blade surface. Figure 1 indicates the transpiration cooling system and its mechanism. The transpiration cooling is composed of two heat exchange processes: the convective one between coolant and the surface of pores included in the porous wall, and the film one over the wall surface. The benefit of this system is the better cooling efficiency with less amount of the coolant compared to the conventional cooling system.

The transpiration cooling system has been applied to the combustor in the rocket engine using fibrous porous and mesh sheets made of stainless steel wire in order to prevent the temperature increase for instance (Ref 12). However, its high-temperature resistance property is very poor for the application to gas turbine blade. On the other hand, heat transfer and fluid numerical analysis was performed extensively (Ref 13-19). The numerical analysis revealed that the cooling efficiency in transpiration cooling is superior to that of film cooling. Thus, in order to establish the transpiration cooling system as the practical technology applicable to the gas turbine blade, the new porous wall materials with high-temperature resistance needs to be developed.

In this study, a porous ceramic coating as the role of the porous wall in the transpiration cooling system is developed with atmospheric plasma spraying which is widely used for stationary gas turbine. The benefits of the ceramic coating application are following: the metal components temperature could be reduced with a low thermal conductivity of ceramic material for which high porosity is introduced, and ceramic material has a stability of the microstructure and a high durability for a long term under high-temperature environment.

In this paper, some properties such as gas permeability, elastic modulus, thermal conductivity, and adhesion strength of the porous ceramic coating developed herein

M. Arai, Materials Science Research Laboratory, Central Research Institute of Electric Power Industry, 2-6-1 Nagasaka, Yokosuka-shi, Kanagawa-ken 240-0196, Japan; and **T. Suidzu**, Thermal Spraying Technology R&D Laboratories, TOCALO Co., Ltd, 14-3, Minamifutami, Futami-cho, Akashi-shi, Hyogo-ken 674-0093, Japan. Contact e-mail: marai@criepi.denken.or.jp.

are shown in comparison with the conventional TBCs used for gas turbine blades. The surface temperature reduction by using the porous ceramic coating under the transpiration cooling is verified by simulation test of the surface temperature distributions of the coated plate samples subjected to a hot gas stream.

2. Experimental Procedure

2.1 Porous Ceramic Coating Deposition

In this study, the mixture of 8 wt.% yttria-stabilized zirconia (204NS-G, Sulzer Metco(Japan), Osaka, Japan) with 10 wt.% content of polyester powders were prepared as feedstock material for the top coat deposition. Figure 2 indicates SEM image of the mixed powder described above. The polyester powder size is somewhat smaller in comparison with the ceramic powders.

The bond coat is CoNiCrAlY (AMDRY 9954, Sulzer Metco(Japan), Osaka, Japan) utilized usually in current gas turbine blade. Prior to deposition of the bond coat, the substrate surface was grit-blasted with white alumina (#54, 0.4 MPa). After the blasting treatment, CoNiCrAlY bond coat was deposited by atmospheric plasma spray system (Unicoat console with an F4MB gun, Sulzer Metco(Japan), Tokyo, Japan) under the well-known spray
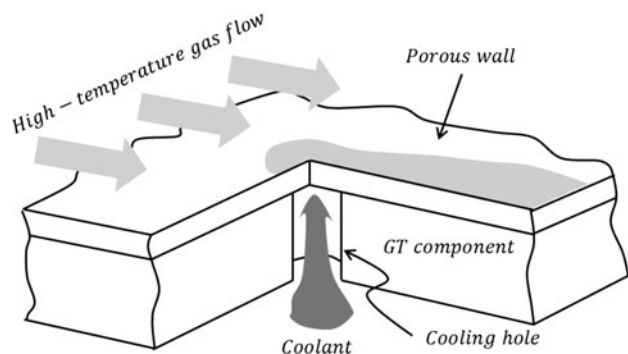
condition in the gas turbine blade. The top coat was then deposited onto the bond coat surface under the optimum spray condition which was confirmed by adjusting particle velocity, substrate temperature, and spray distance for achieving higher porosity and adhesion strength. Spray parameters are listed in Table 1. Here, inflight-particle characteristics were identified using the AccuraSpray (Tecnar Automation Ltd, St. Bruno, QC, Canada). It should be noticed that the particle velocity selected in this process is quite low, but the particle temperature is kept in comparison with the characteristic known in conventional TBCs. After all the deposition processes, the post-heat treatment (2 h at 1073 K) was conducted to evaporate all polyester particles included in the top coat microstructure. Consequently, the open pores can be formed through this evaporation process, and we can have the complete porous ceramic coating.

Figure 3 indicates SEM image of a cross section of the top coat in both conventional TBC and the porous ceramic coating. It can be recognized that the microstructure of the porous ceramic coating includes large open pores and micro cracks linking between pores, which might have the role of a cooling air paths. Zhang et al (Ref 20) also tried to fabricate porous ceramic coating, and for doing it they controlled powder size to form large open pores in the microstructure of the top coating. They reported that pores with average size of 20 μm were formed by employing large particle size powder, which corresponded to a porosity of 22%. For this result, the pores observed in our porous ceramic coating reached size over 100 μm. Porosity associated with our coating will be discussed in latter chapter.

Fig. 1 Schematic representation of the transpiration cooling system for a high-temperature component in gas turbine
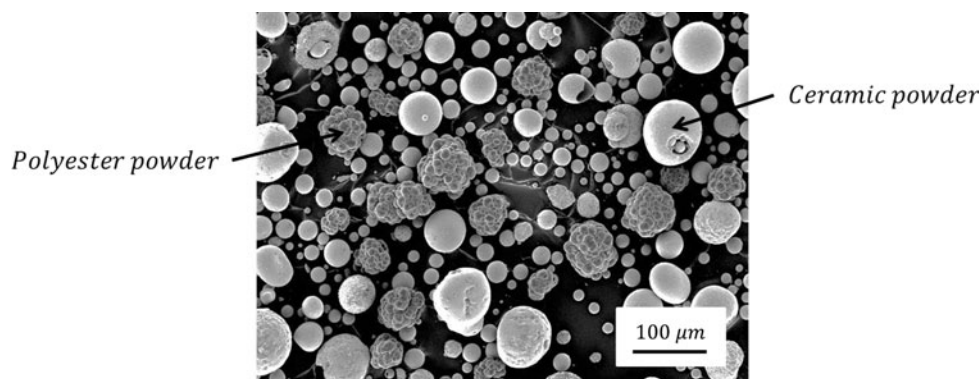
Table 1   Spraying parameters for the top coat

Parameters	Value
Plasma gas	$Ar + H_2$
Power, kW	22
Spray distance, mm	120
Particle velocity, m/s	71
Particle temperature, K	2234
Substrate temperature, K	424

Fig. 2 SEM image of mixed powder employed in this study

2.2 Properties of Porous Ceramic Coating

In this study, the coating properties of the developed coating such as thermal conductivity, porosity, elastic modulus, and interfacial adhesion strength are examined.

Thermal conductivity λ_{coat} of the ceramic coating was measured based on the one-dimensional steady heat flux method. The freestanding coating sample in the form of thin plate peeled from the coated plate using chemical treatment was prepared. The measurement was made by a hand-made device. The device was composed of the following laminated structure: the freestanding coating sample was placed between Cu and Cu thin plates (0.5 mm in thick) for reducing thermal resistance at the contact area between heater panel and the coating sample. Pure Ni thin plate, of which thermal conductivity is known beforehand, was put on the surface of the Cu conductor. This Ni plate has the role of monitoring one-dimensional heat flux along the coating sample thickness. The heat flux was estimated from the temperature drop (ΔT_{Ni}) which was measured from small-gage thermocouples installed in the surface and the rear side of the Ni plate. The ceramic heater panel was put on the other surface of the Cu conductor, and was controlled precisely by PID controller
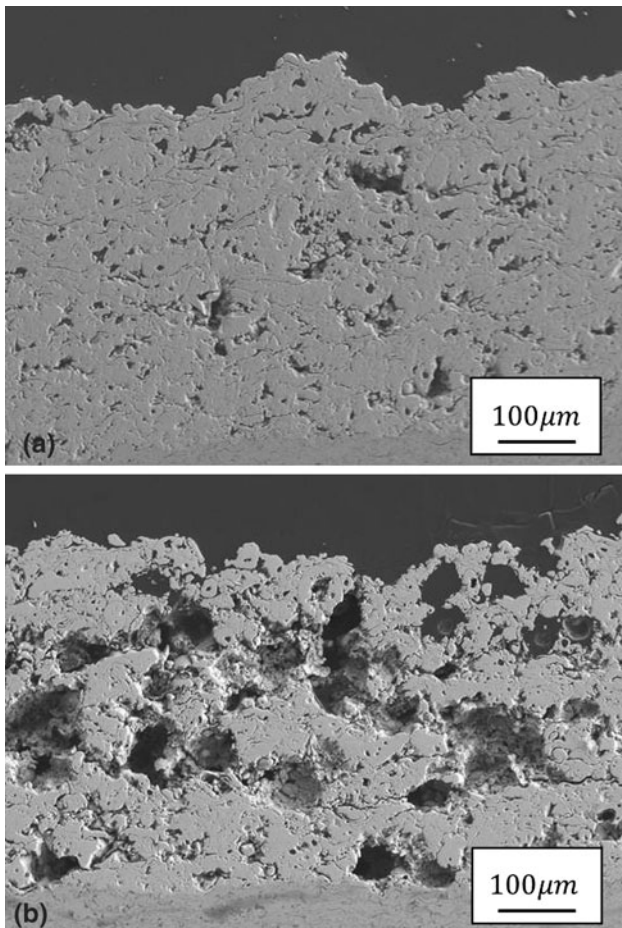

Fig. 3 Microstructure of the ceramic coatings: (a) thermal barrier coating, (b) porous ceramic coating

through thyristor regulator. Thermal conductivity of the porous ceramic coating sample was estimated using the following formula:

$$\lambda_{coat} = \left(\frac{t}{t_{Ni}}\right)\left(\frac{A}{A_{Ni}}\right)\left(\frac{\Delta T_{Ni}}{\Delta T}\right)\lambda_{Ni} \qquad \text{(Eq 1)}$$

where λ_{Ni} is thermal conductivity of pure Ni plate, t is the coating sample thickness, t_{Ni} is Ni plate thickness, A is the contact area of the coating sample on the Ni plate with apparent area A_{Ni}, and ΔT is the temperature drop in the coating sample.

Porosity of the freestanding porous ceramic coating was assessed by measuring the weight of the freestanding coating sample using the electric balance device (EL-1200HA, Shimadzu, Kyoto, Japan). The coating sample used for thermal conductivity measurement was reused.

Elastic modulus of the freestanding porous ceramic coating was evaluated based on the modal analysis carried out in the resonance tester (DEM-11H, Kyoto electronics, Kyoto, Japan). The freestanding coating sample was prepared by the following process: the coated plate substrate was cut in geometry of 130×10 mm by machining, and the freestanding coating was peeled by chemical treatment.

Indentation test (Ref 21, 22) was introduced for evaluating the adhesion strength of the porous ceramic coating. A cross section of the coated sample fixed in the plastic resin was polished up, and then an indenter was indented at the interface between the ceramic and bond coating by using Vickers hardness tester (DVK-2, Matsuzawa, Tokyo, Japan). After removing the indenter from the sample, an interfacial crack is formed along the interface. The adhesion strength was evaluated indirectly from how long the length of crack was. In this study, the indentation load was set at a constant load 98 N and was carried out at room temperature.

2.3 Gas Permeability Test

Figure 4 shows the geometry of the test specimen employed to measure the gas permeability of the porous ceramic coating. The specimen material is Ni-based super alloy IN738LC, and the geometry is a cylindrical shape with a drilled hole with diameter of 6 mm at the center axis, which has the role of passing the cooling air supplied from the reservoir tank in the testing device, but the hole is not penetrated through to the edge of the sample. CoNiCrAlY bond coat is deposited on the edge, and then the small cooling hole with diameter of 2 mm is made at the center of the large cooling hole drilled already with diameter of 6 mm. The plastic bar is inserted to this small cooling hole. The top coat was deposited on the surface of the bond coat. For evaporating plastic bar and all polyester particles included in the deposition, the post-heat treatment was conducted.

Figure 5 shows the hand-made testing device used in this experiment. The atmosphere over the coating surface was heated by an electric furnace up to the maximum temperature of 1473 K. The heat poured into the coating surface by the electric furnace is transferred to the

cylindrical-shaped substrate and then to the jig for fixing the test specimen which has the role of a heat sink. Temperature distribution along the specimen axis can be controlled easily by adjusting temperature of coolant supplied from the cooler to the jig. In the test, the cooling air is injected from the cooling hole in the cylindrical substrate to the porous ceramic coating under a constant pressure P. Temperature distribution in the coated sample, cooling air pressure and flow Q were recorded continuously on PC via A/D converter.

The gas permeability K was assessed by the following relation.

$$K = \frac{\dot{Q}t}{PA_{\text{hole}}} \qquad \text{(Eq 2)}$$

where A_{hole} is the area of air passing through from the cooling hole in the specimen.
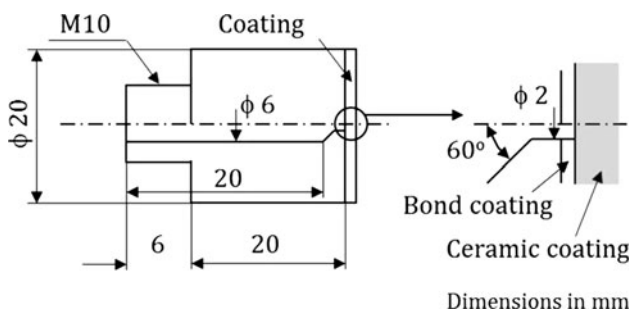

Fig. 4 Specimen geometry employed in this study

2.4 Transpiration Cooling Test

Figure 6 shows the geometry of the plate-shaped specimen employed for transpiration cooling test. The substrate is stainless steel SUS304, and three cooling holes with diameter of 4 mm were drilled at positions A, B, and C but the holes are not completely drilled through the plate. CoNiCrAlY bond coat was deposited up to thickness of 0.1 mm on the side opposite to the drilled holes, and the small hole with diameter of 2 mm was drilled along the center of large cooling hole with diameter of 4 mm drilled already in the substrate. In this test, hole A and holes from A to C were penetrated in order to examine the influence of the number of cooling holes on
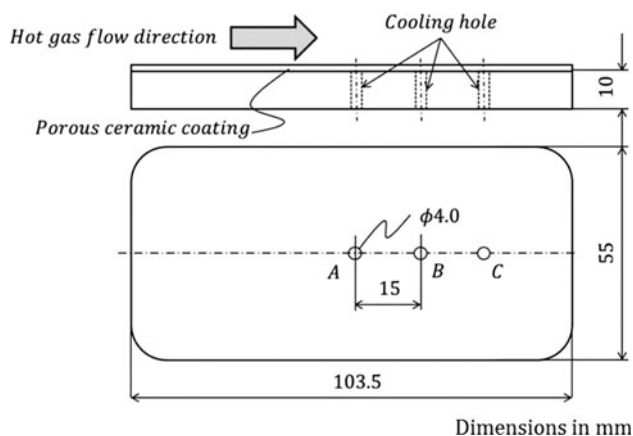

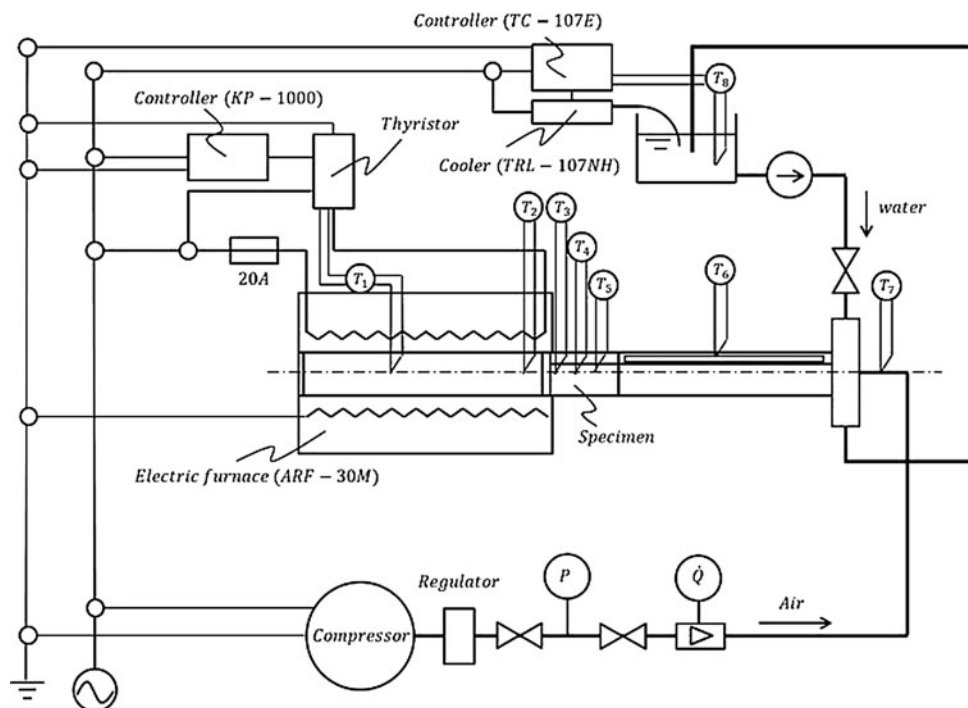Fig. 6 Specimen geometry used for the transpiration cooling test

Fig. 5 Experimental set-up of the testing device employed to measure gas permeability

the cooling efficiency. Those penetrated holes were closed by inserting a plastic bar. Finally, porous ceramic coating with thickness 0.5 mm was deposited on top of the bond coat, and the post-heat treatment was carried out for evaporating all plastic material.

Figure 7 shows the experimental device prepared to conduct transpiration cooling test which could simulate gas stream around a gas turbine blade in laboratory. This transpiration cooling test consists of the follow: a gas is heated up by an electric furnace which was set in front of the sample holder as shown in Fig. 7, and the hot gas of the temperature T_a is streamed with gas velocity v_a on the surface of the plate-shaped sample using the blower. The coolant air pressure P is supplied to the cavity attached to the rear of the sample by the compressor, and it is passed from the cooling hole to the hot gas stream via the porous ceramic coating. The gas velocity was measured using the Pitot tube, and the temperature of the streaming hot gas was measured by thermocouple. The temperature distribution of coating surface was monitored by thermography (Thermo Viewer JTG-6100, JEOL, Tokyo, Japan) which was set up above the sample plate through the view window as shown in Fig. 7. The test condition was set: the inlet hot gas temperature at $T_a = 473$ K and the associated average velocity at $v_a = 4.0$ m/s. Assuming that characteristic length is $L = 0.1$ m, which corresponds to sample length, and kinematic viscosity $\upsilon = 38.58 \times 10^{-6}$ m^2/s, Reynolds number for our hot gas stream field on the plate sample is estimated as $Re = 1.036 \times 10^4$. Thus, the turbulent stream does not occur under this test condition.

3. Experimental Results

3.1 Properties

Figure 8 shows the properties of the porous ceramic coating in comparison with the conventional TBC (hereafter porous ceramic coating is called P-TBC and TBC is called TBC). The plotted data is an average value for experimental data obtained from three specimens. The uncertainty of those data was not so large, however, the number of specimen was insufficient for performing a statistical treatment.
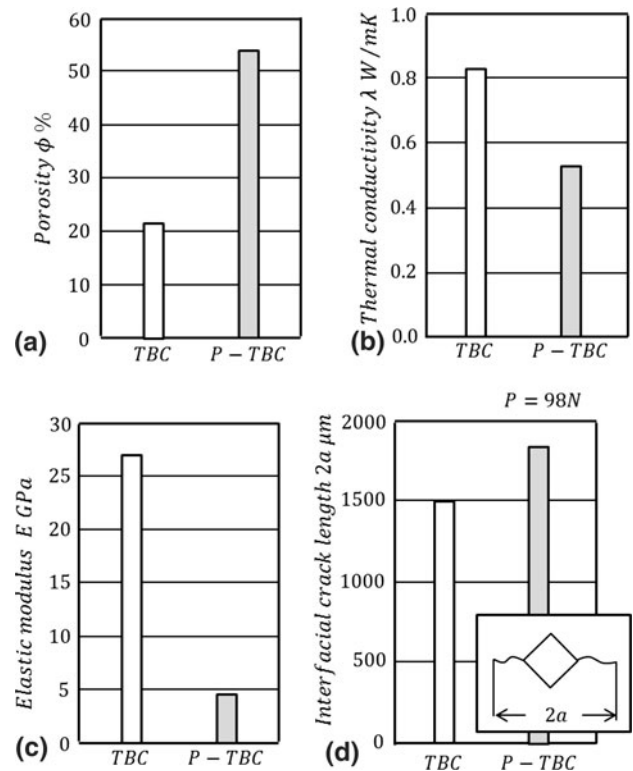

Fig. 8 Comparison in mechanical property between TBC and P-TBC: (a) porosity, (b) thermal conductivity, (c) elastic modulus, (d) adhesion strength
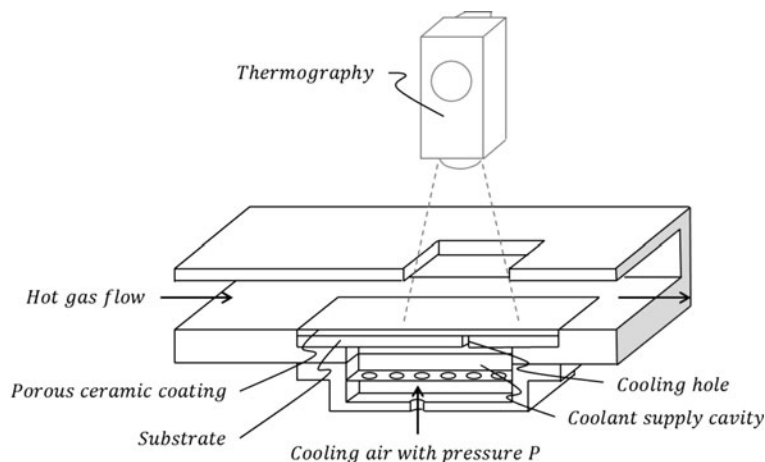

Fig. 7 Experimental set-up of transpiration cooling test under a hot gas flow

Figure 8(a) indicates porosity of P-TBC and TBC. It was found that porosity of P-TBC had higher value than that of TBC. The value for P-TBC porosity was 55% which means that the open pores almost occupy the volume in the ceramic coating. The usage of polyester powder is efficient to form numerous open pores in the deposition.

Figure 8(b) indicates thermal conductivity of P-TBC and TBC. Thermal conductivity of P-TBC is almost half of that of TBC, which takes 0.5 W/mK. It means that P-TBC has superior thermal insulation performance in comparison with the conventional TBC used for gas turbine blade, which is other benefit in P-TBC.

The elastic modulus is shown in Fig. 8(c). The elastic modulus of P-TBC is much lower than that of TBC. Such property of P-TBC was made by large sizes and high density of pores in the microstructure. The low elastic modulus will make thermal stress generated in the coating lower, but it is a weak point for cracking strength. For examining about the cracking and delamination life of the porous ceramic coating, thermal cycling test was conducted. It was recognized that the life was over 1000 cycles under thermal cycling condition between minimum temperature 673 K and maximum temperature 1273 K, which means the porous ceramic coating has sufficient strength to apply to gas turbine blade.

The comparison of adhesion strength between P-TBC and TBC is shown in Fig. 8(d). Here, the interfacial crack length along the interface is regarded as the adhesion strength. The comparison result reveals that the adhesion strength of P-TBC is low only 20% compared with TBC in spite of many pores included in P-TBC microstructure.
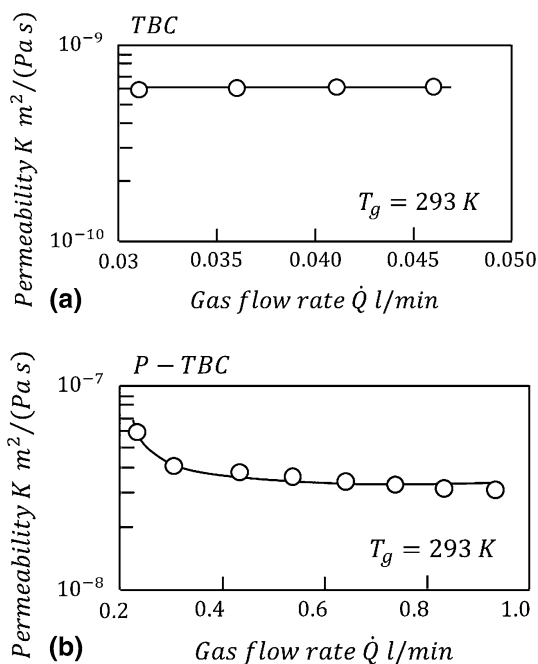
Such adhesion strength might be caused by the post-heat treatment after the thermal spraying process, although the associated mechanisms could not be identified.

3.2 Gas Permeability and Thermal Insulation Performance of Porous Ceramic Coating

Figure 9 shows the variation of cooling gas permeability K with cooling air flow $\dot{Q}$ at room temperature. In the case of TBC, the quantity of little cooling air flows through the coating thickness, which takes constant value as approximately 6×10^{-10} m²/(Pa s) over all cooling air flow range. On the other hand, P-TBC has higher cooling gas permeability, which is 100 times as much as TBC. This means that the porous ceramic coating has excellent capability for application to the transpiration cooling. However, the trend in the permeability decreases with the
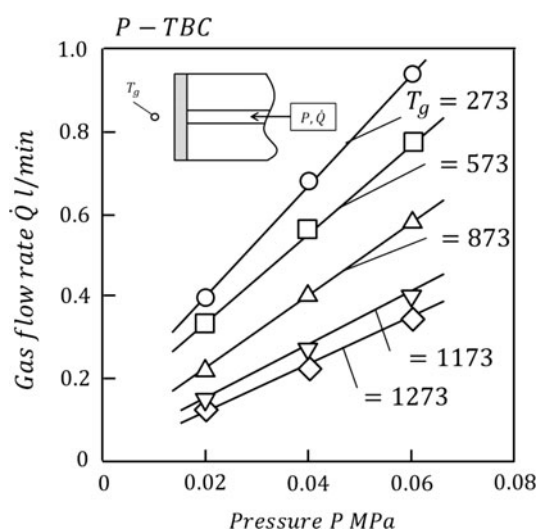

Fig. 10 Relationship between gas flow rate and pressure

Fig. 9 Variation of permeability with gas flow rate at room temperature: (a) thermal barrier coating, (b) porous ceramic coating
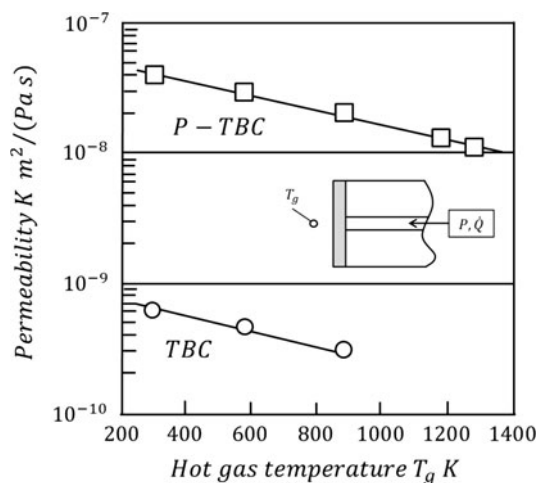

Fig. 11 Variation of permeability with hot gas temperature around the coating surface

increase of cooling air flow. It indicates the importance of viscous flow and friction on the pore surface when cooling air flows via pores and microcracks in the microstructure.

Figure 10 indicates the relationship between cooling air flow and the pressure P when cooling air is passing across P-TBC. Cooling air flow increases linearly with the
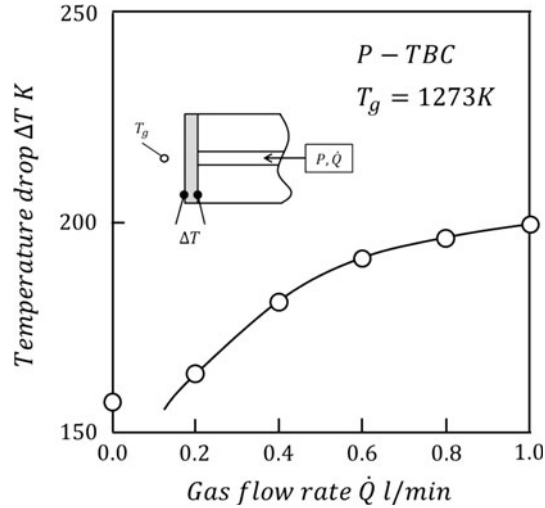
pressure, however, the higher temperature T_g above the coating surface brings about reduction of cooling air flow. The reason for such trend might be brought by the phenomena of air path closing with thermal expansion inside the microstructure.

Figure 11 indicates relationship between the gas permeability and the temperature above the coating surface in comparison between TBC and P-TBC. In the results of P-TBC, the gas permeability decreases monotonously with the increase of the temperature T_g, which means that the optimum value in the cooling air pressure extruded from the combustor should be chosen in order to keep air infiltration via the porous ceramic coating at a high-temperature environment. For this trend as seen in P-TBC, value of gas permeability is much lower in TBC, but has a linear trend to hot gas temperature.

Figure 12 indicates thermal insulation performance of P-TBC at the temperature $T_g = 1273$ K above the top coat surface. Here, the plotted data is an average value for experimental data obtained from three specimens. It is found that temperature drop between the near-surface of the top coat and the interface between top and bond coat increases with the amount of cooling air flow. It seems that temperature drop will be saturated if cooling air flow becomes large. It can be recognized that porous ceramic coating has an excellent performance for thermal insulation and can control the temperature drop by adjusting cooling air pressure or flow.
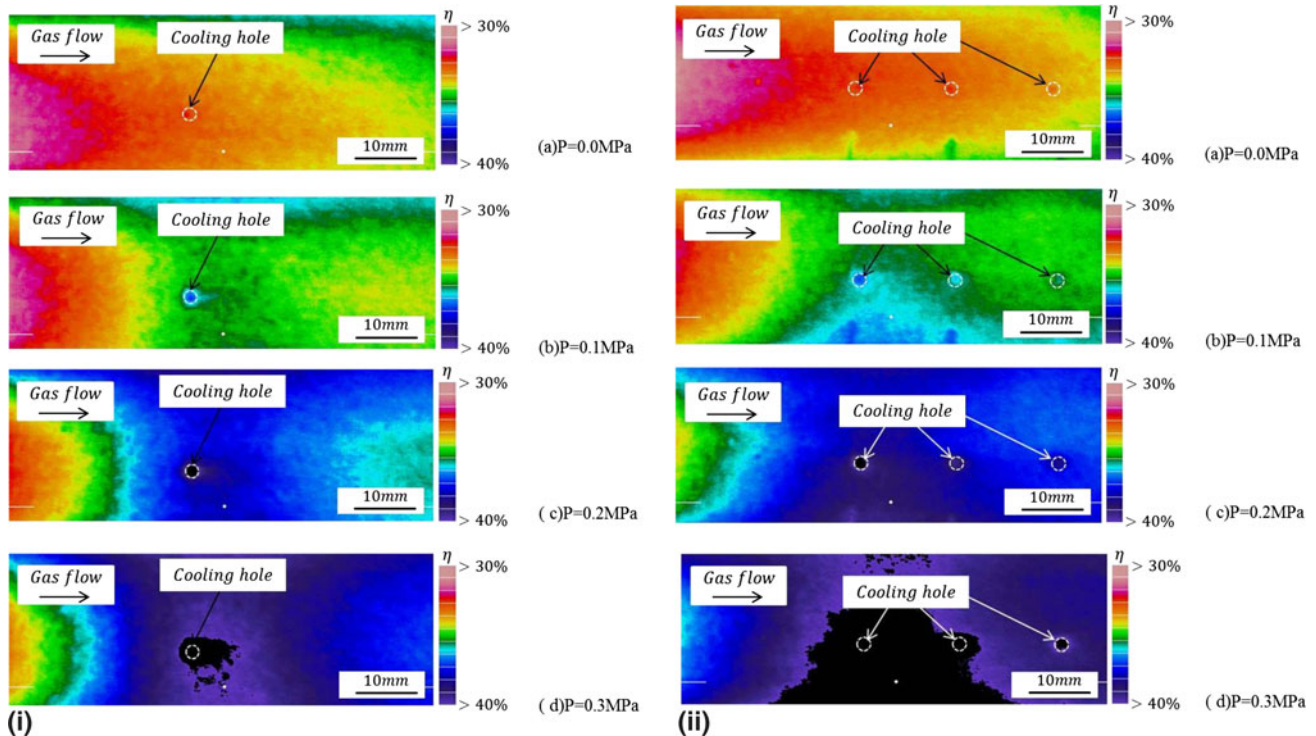

Fig. 12 Thermal insulation performance with the increase of gas flow rate
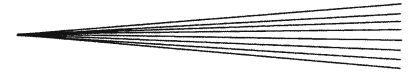

Fig. 13 Cooling efficiency η on the coating surface subject to the hot gas flow (a) $P = 0.0$ MPa, (b) $P = 0.1$ MPa, (c) $P = 0.2$ MPa, (d) $P = 0.4$ MPa, (i) in the case of cooling hole opened at A (a) $P = 0.0$ MPa (b) $P = 0.1$ MPa (c) $P = 0.2$ MPa (d) $P = 0.4$ MPa (ii) in case of the cooling hole opened from A to C

3.3 Cooling Effect of Transpiration Cooling System with Porous Ceramic Coating

Figure 13 indicates the cooling efficiency η distribution on the surface of the coating plate sample which was measured by thermography. Here, the cases in cooling air pressure P of 0, 0.1, 0.2, and 0.3 MPa are shown in order to verify the transpiration cooling system using porous ceramic coating. The cooling efficiency used in this study is defined by,

$$\eta = \frac{T_a - T_c}{T_a} \qquad \text{(Eq 3)}$$

where T_c is the surface temperature of the coated plate-shaped sample. It should be noticed that the definition used here is different from the definition for the cooling efficiency generally known in gas turbine blade design. Usage of this definition makes it easy to understand how surface temperature fell from hot gas temperature. It is indicated that the hot gas flows from left to right direction on the figures, and the efficiency η increases from red to blue color. The results reveal that the area on which the surface temperature falls concentrated on the cooling hole spreads concentrically with the increase of cooling air pressure and then spreads along the hot gas stream. It means that the cooling air is infiltrated through the porous coating wall and is also diffused inside the porous coating structure concentrically, which associates with the convective heat exchange process between cooling air and the surface of the pores in the porous coating. The cooling area expanding along the hot gas flow accelerates the film cooling process.

The increase of the number of cooling holes brings about the more area of surface temperature reduction. Those observation results verify the validity of transpiration cooling system combined with the porous ceramic coating for gas turbine blade.

4. Conclusion

In this study, the porous ceramic coating for the transpiration cooling system in gas turbine blade was developed using atmospheric plasma spray process that is generally used to protect current gas turbine blades from the high-temperature gas flow. The coating was composed of 8 wt.% yttria-stabilized zirconia and polyester powder mixture. Later the polyester powder was evaporated by the post-heat treatment. The coating properties were examined. The porous ceramic coating indicated a low thermal conductivity, which was one-half of TBCs, and had adhesion strength low only 20% compared with TBC. Thermal insulation of porous ceramic coating by infiltrating cooling air indicated an excellent performance, and increased the temperature drop above the coating with cooling air pressure. Finally, it was found that the coating surface temperature was reduced and the temperature dropped concentrically around a cooling hole by performing transpiration cooling test as simulating gas stream field around gas turbine blade. Thus, the transpiration cooling system combined with the porous ceramic coating for gas turbine blade was verified to be very effective for cooling gas turbine blade.

References

1. R.V. Hillery, N. Bartleti, H.L. Bernstein, R. Davis, H. Herman, L. Hsu, J.C. Murphy, R.A. Rapp, J.S. Smith, and J. Stringer, *Coatings for High-Temperature Structural Materials Trends and Opportunities*, National Academy Press, Washington, DC, 1996, p 10-18
2. J.X. Zhang, T. Murakami, H. Harada, and Y. Koizumi, Dependence of Creep Strength on the Interfacial Dislocations in a Fourth Generation SC Superalloy TMS-138, *Scripta Mater.*, 2003, **48**, p 287-293
3. Z.X. Zhang, H. Harada, Y. Ro, Y. Koizumi, and T. Kobayashi, Thermomechanical Fatigue Mechanism in a Modern Single Crystal Nickel Base Superalloy TMS-82, *Acta Mater.*, 2008, **56**, p 2975-2987
4. Z.X. Zhong, Y. Gu, Y. Yuan, T. Yokokawa, and H. Harada, Mechanical Properties and Fracture Modes of an Advanced Ni-Co-Base Disk Superalloy at Elevated Temperatures, *Mater. Charact.*, 2012, **67**, p 101-111
5. U. Schulz, C. Leyens, K. Fritsher, M. Peters, B. Saruha-Brings, O. Lavigne, J.-M. Dorvaux, M. Poulain, R. Mevrel, and M. Caliez, Some Recent Trends in Research and Technology of Advanced Thermal Barrier Coatings, *Aerospace Sci. Technol.*, 2003, **7**, p 73-80
6. D.R. Clarke and S.R. Phillpot, Thermal Barrier Coating Materials, *Mater. Today*, June, 2005, p 22-29
7. Sanjay, O. Singh, and B.N. Prasad, Influence of Different Means of Turbine Blade Cooling on the Thermodynamic Performance of Combined Cycle, *Appl. Therm. Eng.*, 2008, **28**, p 2315-2326
8. Sanjay, O. Singh, and B.N. Prasad, Comparative Performance Analysis of Cogeneration Gas Turbine Cycle for Different Blade Cooling Means, *Int. J. Therm. Sci.*, 2009, **48**, p 1432-1440
9. V.M. Polyaev, A.P. Mozhaev, B.M. Galitseysky, and A.L. Lozhkin, A Study of Internal Heat Transfer in Nonuniform Porous Structures, *Exp. Therm. Fluid Sci.*, 1996, **12**, p 426-432
10. G. Cerri, A. Giovannelli, L. Battisti, and R. Fedrizzi, Advances in Effusive Cooling Techniques of Gas Turbines, *Appl. Therm. Eng.*, 2007, **27**, p 692-698
11. E. Lugscheider, K. Bobzin, A. Etzkorn, A. Horn, R. Weichenhain, E.W. Kreutz, and R. Poprawe, Electron Beam-Physical Vapor Deposition—Thermal Barrier Coatings on laser Drilled Surfaces for Transpiration Cooling, *Surf. Coat. Technol.*, 2000, **133**, p 49-53
12. E. Sozer and W. Shyy, Modeling of Fluid Dynamics and Heat Transfer Through Porous Media for Liquid Rocket Propulsion, *Proceedings of 43rd AIAA/ASME/SAE/ASEE Joint Propulsion Conference & Exhibit*, July 8-11 (Cincinnati, OH), 2007, p 1-11
13. J. Polezhaev, The Transpiration Cooling for Blades of High Temperatures Gas Turbine, *Energy Conv. Manag.*, 1997, **38**(10-13), p 1123-1133
14. C. Trevino and A. Medina, Analysis of the Transpiration Cooling of a Thin Porous Plate in a Hot Laminar Convective Flow, *Eur. J. Mech. B/Fluid*, 1999, **18**(2), p 245-260
15. G. Laschet, Homogenization of the Fluid Flow and Heat Transfer in Transpiration Cooled Multi-layer Plates, *J. Comput. Appl. Math.*, 2004, **168**, p 277-288
16. A.Z. Weber and J. Newman, Modeling Gas-Phase Flow in Porous Media, *Int. Commun. Heat Mass Transfer*, 2005, **32**, p 855-860
17. A.A. Alshare, P.J. Strykowski, and T.W. Simon, Modeling of Unsteady and Steady Fluid Flow, Heat Transfer and Dispersion in Porous Media Using Unit Cell Scale, *Int. J. Heat Mass Transfer*, 2010, **53**, p 2294-2310
18. W.-L. Chen and Y.-C. Yang, Simultaneous Estimation of Heat-Transfer Rate and Coolant Fluid Velocity in a Transpiration Cooling Process, *Int. J. Therm. Sci.*, 2010, **49**, p 1407-1416
19. F.R. Villatoro, J. Perez, J.L.G. Santander, M.A. Borovsky, Y.L. Ratis, E.A. Izzheurov, and P. Fernandez de Cordoba, Perturbation Analysis of the Heat Transfer in Porous Media with Small Thermal Conductivity, *J. Math. Anal. Appl.*, 2011, **374**, p 57-70
20. C. Zhang, W.-Y. Li, M.-P. Planche, C.-X. Li, H. Liao, C.-J. Li, and C. Coddet, Study on Gas Permeation Behavior Through Atmospheric Plasma-Sprayed Yttria Stabilized Zirconia Coating, *Surf. Coat. Technol.*, 2008, **202**, p 5055-5061

21. D. Chicot, P. Demarecaux, and J. Lesage, Apparent Interface
Toughness of Substrate and Coating Couples from Indentation
Tests, *Thin Solid Films*, 1996, **283**, p 151-157

22. M. Arai, Interfacial Fracture Toughness Evaluation of Ceramic
Thermal Barrier Coatings Based on Indentation Test Method, *J.
Soc. Mater. Sci.*, 2009, **58**(11), p 917-923 (in Japanese)